


 Cite this: *RSC Adv.*, 2020, **10**, 11182

# Controllable synthesis of *in situ* grown titanate hierarchical microspheres and subsequent chemical modifications for superhydrophobic and oil–water separation properties<sup>†</sup>

 Yong Li,<sup>‡,a</sup> Jiyang Xie,<sup>‡,a</sup> Changjin Guo,<sup>a</sup> Jian Wang,<sup>\*,b</sup> Huan Liu<sup>a</sup> and Wanbiao Hu<sup>ID, ab</sup>

Sodium titanate nanowire-assembled microspheres on titanium mesh have been synthesized through controlling an over the surface acidification and hydrothermal process in terms of a proposed *in situ* “nucleation-cum-growth” solution chemistry strategy. These directly grown microspheres crystallize in an orthorhombic lepidocrocite layered structure of sodium titanate with the composition of  $\text{Na}_{1.8}\text{Ti}_{1.95}\square_{0.05}\text{O}_{4.8}$  ( $\square$  ~ vacancy) determined by the XRD, Raman and SEM-EDX techniques. An individual microsphere has a uniform size of around 10 microns while the constituent nanowires have a diameter of 100 nm growing along the [110] orientation. Owing to the specially well-defined hierarchical structure and robust *in situ* interfaces, these titanate nanowire-assembled microspheres, after 2,2,3,3,4,4,5,5-octafluoro-1-pentanol (OFP) surface modification, could achieve superhydrophobicity. This work demonstrates an *in situ* “nucleation-cum-growth” synthesis strategy and facile functionalization towards superhydrophobicity for oil–water separation, which might extend to a broad variety of oxide nanowire systems to fabricate well-defined structures for wettability tailoring and multi-functional applications.

 Received 14th January 2020  
 Accepted 5th March 2020

DOI: 10.1039/d0ra00381f

[rsc.li/rsc-advances](http://rsc.li/rsc-advances)

## 1. Introduction

Nowadays, oily wastewater that originates from daily and industrial sewerage is becoming a severe environmental issue that is increasingly threatening human health.<sup>1–5</sup> It is rather urgent to develop effective and economically-friendly approaches, on the one hand for cleaning up oil–water mixture, and on the other for saving resources through oil purification and recycling from oily wastewater. Although various methods and techniques *e.g.* centrifuges,<sup>6</sup> depth filtrations,<sup>7</sup> skimming and oil-absorbing materials *etc.*<sup>2,8,9</sup> have been extensively explored, a simple, efficient and economic strategy to directly filtrate oil from oily wastewater is still required.

A membrane material with simultaneously hydrophobic (or hydrophilic) and oleophilic (or oleophobic) features might be an attractive solution.<sup>1,3,8,10–12</sup> Traditional polymer-based materials have been well utilized in this regard, for instance polyvinylidene fluoride (PVDF),<sup>3,13,14</sup> poly(methacrylic acid-*co*-ethylhexylmethacrylate) (PMAA-*co*-EHMA)<sup>15</sup> and poly(*N*

isopropylacrylamide) (PNIPAM) complex *etc.*,<sup>16,17</sup> but they suffer from the relatively low thermal stability, chemical resistance, mechanical strength. An appealing alternative could be inorganic-based materials with robust pores to achieve controllable surface wettability by tailoring their well-defined structures and meanwhile applying an external stimuli. This evokes a large number of endeavours to develop artificial structures *e.g.* well-aligned arrays, patterns and hierarchical structures *etc.* However, construction of these structures requires complicated processing and high costs. Furthermore, the microstructural stability issues are still opening because of the weak contact robustness.<sup>18,19</sup>

A much more facile route, *i.e.* an *in situ* solution chemistry that allows a well-defined structure directly growing on a porous substrate,<sup>20</sup> is scientifically promising. This furthermore facilitates the formation of a Cassie state,<sup>21</sup> *i.e.* an air layer between the water and the surface, which is necessary for achieving a superhydrophobic surface. As a result, a solution-favored hierarchical surface might be an effective strategy because such type of surface can provide the particular surface structures and roughness. Through simply surface modifications, a low free energy state would be obtained. This is supported by the fact that hierarchical surfaces have been extensively adopted to enhance the Cassie state stability.

To address the aforementioned issues, we proposed an *in situ* “nucleation-cum-growth” solution chemistry route to synthesize

<sup>a</sup>Key Laboratory of LCR Materials and Devices of Yunnan Province, School of Materials Science and Engineering, Yunnan University, Kunming 650091, P. R. China

<sup>b</sup>School of Physics and Astronomy, Yunnan University, Kunming 650091, P. R. China.  
E-mail: wangjian@ynu.edu.cn

† Electronic supplementary information (ESI) available. See DOI: 10.1039/d0ra00381f

‡ These authors equally contribute to this work.



titanate nanowire-assembled hierarchical microspheres on titanium mesh based on the following considerations: (i) titanium metal has superior chemical stability and mechanical strength that render the titanium mesh ideal for standing hydrophobic structures; (ii) one-dimensional titanate nanostructures can be solution-chemistry formed under alkaline conditions, which makes the nanowires *in situ* synthesis and further development into hierarchical microspheres possible through controlling the primary nucleation properly;<sup>20,22</sup> (iii) titanium-based oxides *e.g.*  $\text{TiO}_2$  and titanate can be easily surface modified to achieve robust superhydrophobicity,<sup>23,24</sup> thus giving rise to the effective oil/water separation combined with the titanium mesh substrate. With regard to realizing the hydrophobicity state, it is noted that the fluorum–carbon groups have relatively small surface tension, *e.g.* 23 dyn  $\text{cm}^{-1}$  for  $\text{CF}_2$ , which have been extensively used to lower the surface energy. What's more, because nearly all the oxides are hydrated, proper modifiers with OH-end groups may be required to fulfil the surface modification. Taken into these considerations, a hydroxyl/fluorom-containing modifier *i.e.* octafluoro-1-pentanol [ $\text{F}_2\text{CH}(\text{CF}_2)_3\text{CH}_2\text{OH}$ ] (noted as OFP) could be suitable. Bear these in mind, we synthesized titanate nanowire-assembled hierarchical microspheres standing on the titanium mesh by controlling the *in situ* nucleation and growth, which were subsequently surface modified with OFP to realize superhydrophobic for oil/water separation performance.

## 2. Experimental sections

### 2.1 Materials and reagents

The chemicals and reagents used in the experiments are described as follows: Ti metal mesh (99.99%, 200 mesh, Sigma-Aldrich), isopropanol (99.9%, aladdin), ethanol (99.9%, aladdin), HCl (37 wt%, Sinoreagent), NaCl (99.99%, Sinoreagent), NaOH (99.99%, Sinoreagent), 2,2,3,3,4,4,5,5-octafluoro-1-pentanol (99.99%, Sigma-Aldrich). Deionized water ( $\sim$ 18.25 M $\Omega$  cm) was made by the water purifier (AOKLAND). The chemicals were directly used for the experiments without further treatments.

### 2.2 Surface acidification of Ti mesh

A piece of Ti metal mesh (2.5 cm  $\times$  2.5 cm) was thoroughly cleaned by isopropanol, ethanol, and deionized water successively under ultrasonic. The cleaned Ti mesh was vertically placed (fixed by a Teflon shelf) into a Teflon-lined stainless steel autoclave (100 mL volume) which contains a mixed solution (80 mL) of HCl (0.1 M) and NaCl (0.1 M) for solution-chemistry reaction at 160 °C. After reaction for 1 hour, the Ti mesh was taken out from the cooled autoclave and again cleaned by isopropanol, ethanol, and deionized water successively under ultrasonic. After surface acidification, the Ti mesh with etched surfaces could be obtained, which were used for the subsequent hydrothermal reactions.

### 2.3 Hydrothermal reaction for *in situ* nucleation-cum-growth

Firstly, a certain concentration of the NaOH ( $C_{\text{NaOH}}$ ) aqueous solution (80 mL) was transferred into a Teflon-lined stainless

steel autoclave (100 mL volume). Afterward, the etched and cleaned Ti mesh was vertically placed (fixed by a Teflon shelf) into the autoclave for the hydrothermal synthesis. The hydrothermal reaction was conducted at the selected temperatures ( $T_{\text{hydro}}$ ) and durations ( $t_{\text{hydro}}$ , normally 6 h) in an electric oven. The synthesis conditions were well tuned in terms of  $C_{\text{NaOH}}$  (0.01–10 M),  $T_{\text{hydro}}$  (120–200 °C) and  $t_{\text{hydro}}$  (1–10 hours) to obtain the optimal reaction condition. Under the optimal condition, the primary nucleation can be progressed and further develop into the titanate nanowire-assembled hierarchical microspheres standing on the Ti mesh.

### 2.4 Surface modifications for hydrophobicity

To achieve the hydrophobicity for the as-prepared titanate hierarchical microspheres, a fluorine-containing modifier, *i.e.* 2,2,3,3,4,4,5,5-octafluoro-1-pentanol (OFP), was used to modify the microspheres. Typically, the Ti mesh with the titanate hierarchical microspheres standing on was immersed into a mixed solvent of OFP and 2-propanol with a variable concentrations of  $C_{\text{OFP}} = 0.025\text{--}2 \text{ mol L}^{-1}$  at 60 °C. After reaction for 2 h, the surface modifications were finished. The Ti mesh was taken out from the solvent and thoroughly rinsed with deionized water.

### 2.5 Sample characterizations and hydrophobicity measurements

Crystalline structures and phases were characterized by X-ray diffraction (XRD, Rigaku Smartlab) and Raman spectroscopy (Renishaw inVia). Morphologies were imaged by Scanning Electron Microscopy (SEM, Zeiss Gemini500). Crystalline orientations were determined by the transmission electron microscopy (TEM, JEOL JEM-2100F). Fourier transform infrared (FT-IR) spectra were collected on PerkinElmer frontier spectrometers. The surface wettability and hydrophobicity of the titanate nanowire-assembled hierarchical microspheres on Ti mesh was characterized using a KSV CAM200 Goniometer instrument at ambient temperature in air, and the water contact angles (CA) were determined by averaging measurements taken from at least five different positions on the measured Ti-mesh surface.

## 3. Results and discussion

The *in situ* synthesis of titanate hierarchical microspheres standing on titanium (Ti) mesh was schematically proposed in Fig. 1. Ti metal mesh (200 mesh) was firstly etched in a mixed solution of HCl (0.1 M) and NaCl (0.1 M) at 120 °C to allow surface acidification (Fig. 1a and b). The surface Ti could react with  $\text{H}^+/\text{Na}^+$  species at high temperature (160 °C) that makes the originally smooth surface Ti (Fig. 1a) dissolved slightly, leaving the rough surface after etching (Fig. 1b). It is noted that such an initial etching process is essential for subsequently hydrothermal nucleation reaction, because only the homogenous nanowires instead of the hierarchical microspheres could form if no etching treatment (see ESI S1†). When proceeding the subsequent hydrothermal reactions in



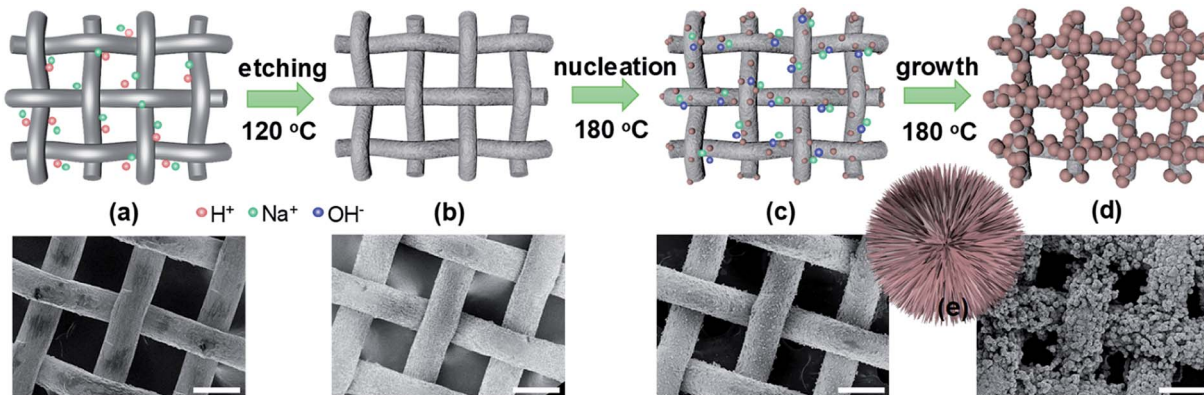


Fig. 1 Proposed solution-chemistry scheme of the *in situ* nucleation-cum-growth procedure for synthesizing the titanate hierarchical microspheres standing on Ti mesh. (a) Fresh Ti mesh; (b) etched Ti mesh; (c) primary titanate nucleation; (d) growth into titanate hierarchical microspheres; (e) a demonstration of a typical nanowire-assembled hierarchical microsphere. The corresponding SEM images for the each stage were also shown. The scale bars in SEM denote 100 micron.

NaOH aqueous solution, these rough surface configurations thus facilitates the inhomogeneous nucleation. The subsequent growth can be completed in 6 h, which starts from a nucleation region (S2†). However, the nucleation and growth processes are closely associated with the NaOH concentration ( $C_{\text{NaOH}}$ ) and temperatures ( $T_{\text{hydro}}$ ) of the hydrothermal reactions.<sup>20</sup> Relatively low  $C_{\text{NaOH}}$  (e.g. below 0.5 M) leads to the very slow nucleation that allows the nucleation occurring nearly homogenous on the Ti surface. As a result, only the titanate nanosheets, nanowires or nanobelts were formed to uniformly cover on the Ti mesh (Fig. S3–S5†). On the contrary, relatively high  $C_{\text{NaOH}}$  (e.g. over 2 M) would result in the very quick nucleation and reaction everywhere. That is, the titanate nucleation and growth not only happen on the Ti surface but also in the solution near the Ti mesh. Therefore, both the microspheres and nanowires distributed disorderly and unevenly on the Ti mesh were generated (S6†). Likewise, relatively low or high  $T_{\text{hydro}}$  (below 160 °C or over 200 °C) would

give rise to the formation of the simultaneous microspheres and nanowires or large bulks (S7 and S8†), which are not uniform either. To conclude, under the conditions of  $C_{\text{NaOH}} \sim 1$  M,  $T_{\text{hydro}} \sim 180$  °C and  $t_{\text{hydro}} \sim 6$  h that govern the optimal nucleation and growth (Fig. 1c and d), the hierarchical microspheres consisting of sodium titanate nanowires standing on titanium (Ti) mesh were synthesized (Fig. 1e).

It is well documented that  $\text{Ti}^{4+}$ -based groups or oxides e.g.  $\text{TiO}_2$  can react with NaOH to form sodium titanate nanostructures, but the resulting crystal structures are often complicated and debated.<sup>22</sup> Here, XRD and Raman were performed to identify the phase structure. As shown from XRD (Fig. 2a), in addition to the Ti-mesh substrate, all the diffraction lines can be indexed to a layer-structured titanate. Raman spectra (Fig. 2b and S9†) present mainly 5 peaks at 282, 439, 641, 712 and 903  $\text{cm}^{-1}$ , respectively, which match well the orthorhombic layered lepidocrocite titanate with a basic skeleton of  $\text{A}_{2-x}\text{Ti}_{2-x/4}\square_{x/4}\text{O}_{4+\Delta}$  ( $\square \sim$  vacancy).<sup>25,26</sup> This is

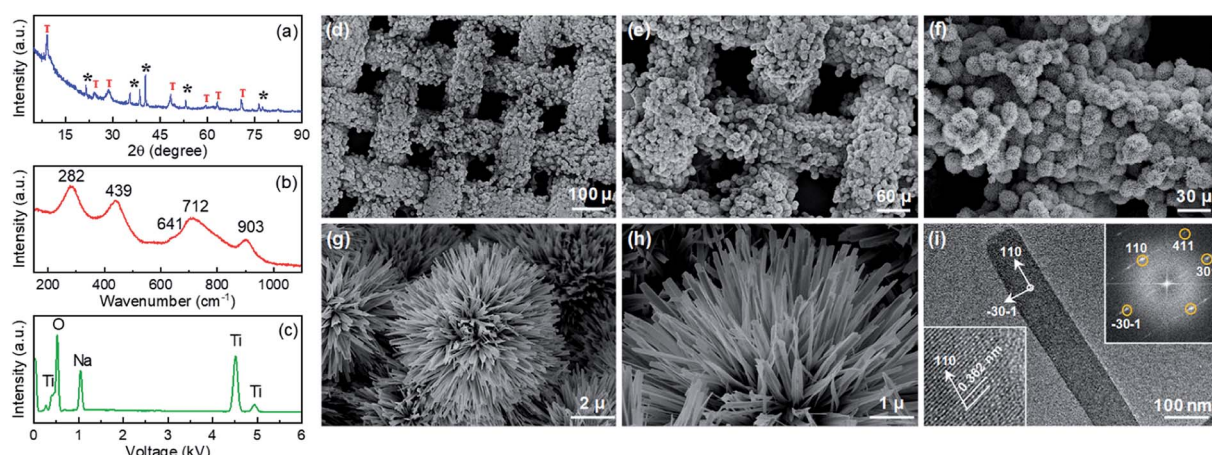


Fig. 2 Phase and microstructure characterizations of the as-synthesized titanate hierarchical microspheres. (a) XRD pattern; (b) Raman spectrum; (c) EDX spectrum collected by SEM observation; (d–h) FESEM images under different magnifications; (i) TEM images with the inset HRTEM and FFT images. The symbols "T" in (a) denote the characteristic diffraction peaks of the layer-structured titanate while asterisks \* denote the diffraction lines from the Ti-metal mesh.



a protonic-acid based titanate with A-site exchangeable by protons and alkaline cations. Under the conditions of existing NaOH, sodium titanate was expected, as evidenced by SEM-EDX determinations (Fig. 2c and S10† that demonstrates the EDX spectra collected at different areas), which give a Na/Ti atomic ratio of around 0.92. Thus, the composition for present lepidocrocite titanate could be estimated to be  $\text{Na}_{1.8}\text{Ti}_{1.95}\square_{0.05}\text{O}_{4.8}$  ( $\square \sim \text{vacancy}$ ).

The microstructures of the as-synthesized titanate hierarchical microspheres were further carefully characterized by electron microscopy. As shown in Fig. 2d-f, the microspheres were evenly and uniformly grown on the Ti mesh. An individual microsphere has a typical diameter of around 10 microns and is composed of smaller nanowires with the sectional dimension of near 100 nm (Fig. 2g and h), which together with the Ti-mesh substrate forms the hierarchical structure. Careful observation reveals that these nanowires, at the initial stage of the hydrothermal reaction, all grew from a common region. That is, they shared a same nucleation and subsequently developed into the microsphere in terms of evenly growing in all the direction when prolonging the hydrothermal durations, consistent with the proposed “nucleation-cum-growth” mechanism in Fig. 1c and d. The nanowire shows the well crystalline state (HRTEM in Fig. 2i-inset) in an orthorhombic structure, with a growth orientation along [110] direction confirmed by the HRTEM and fast Fourier transform (FFT) pattern (Fig. 2i-inset).

A straightforward demonstration of the functional superiority for the titanate hierarchical microspheres standing on Ti mesh currently is the simple surface modification towards superhydrophobicity. To reach this end, a fluorine-containing modifier 2,2,3,3,4,4,5,5-octafluoro-1-pentanol (OFP) was used for simply surface functionalization because the substituent end-groups  $\text{CF}_2$  have a relatively small surface tension of only  $23 \text{ dyn cm}^{-1}$ .<sup>27</sup> Specifically, the Ti mesh with microspheres standing on was immersed into the 2-propanol solution with a certain concentration of OFP at  $60^\circ\text{C}$  for 12 h, which was confirmed by FT-IR (S11†). Fig. 3 shows the wettability properties of the OFP-modified titanate hierarchical microspheres

on Ti mesh, where the titanate nanostructures synthesized at different  $C_{\text{NaOH}}$  were also compared. It is clear that the titanate nanostructures synthesized at low NaOH concentration ( $C_{\text{NaOH}} \sim 0.01 \text{ M}$ ) shows the hydrophilic feature while a slight increase in  $C_{\text{NaOH}}$  could give the hydrophobic feature, *e.g.* at  $C_{\text{NaOH}} = 0.1 \text{ M}$ , the resulting contact angle (CA) measured can be up to  $105^\circ$ . Further increasing the  $C_{\text{NaOH}}$  could realize the quite high CAs ( $\sim 150^\circ$ ) because the titanate nanostructures have been well developed in hydrothermal reactions under such  $C_{\text{NaOH}}$  conditions. Owing to the specially hierarchical structure, the hierarchical microspheres strikingly show the highest CA of  $153 \pm 1^\circ$ , which was synthesized at  $C_{\text{NaOH}} = 2 \text{ M}$ . Afterwards, the nanowires that assemble into the microspheres gradually develop into the big bulks (S8†), losing the Cassie state. The hydrophobic Cassie state through surface OFP modifications on titanate microspheres also depends on the OFP modifier concentration as indicated in Fig. 3b. Too less OFP amount cannot effectively reduce the surface energy to permit a Cassie state as the surface tension between water is as high as  $72.8 \text{ mN m}^{-1}$ . This can only be done at a certainly high OFP amount of over 5 mL. Therefore, it can be concluded that the chemical modifications govern the hydrophobic states or not, while the morphological structure amplifies this state to superhydrophobic proportions. A scheme is also proposed to demonstrate the possible surface Cassie state with water-OFP-titanate interfaces (Fig. 3b-inset).

The superhydrophobic feature of the OFP-modified titanate microspheres on Ti mesh was fully demonstrated. The water flow can keep running on the Ti mesh surface with neither spreading nor penetrating into the mesh (Fig. 4a and video in ESI V1†). Likewise, the static water droplets can stay on the mesh surface without diffusion, again revealing a relatively large contact angle (Fig. 4a-c). The nearly same superhydrophobic results were also obtained when using salt water (NaCl/KCl mixed solution was performed) instead as clearly shown in Fig. 4d-f (also video in ESI V2†), which thus are potential for sea-water related applications. The superhydrophobic mesh was furthermore exemplified to demonstrate

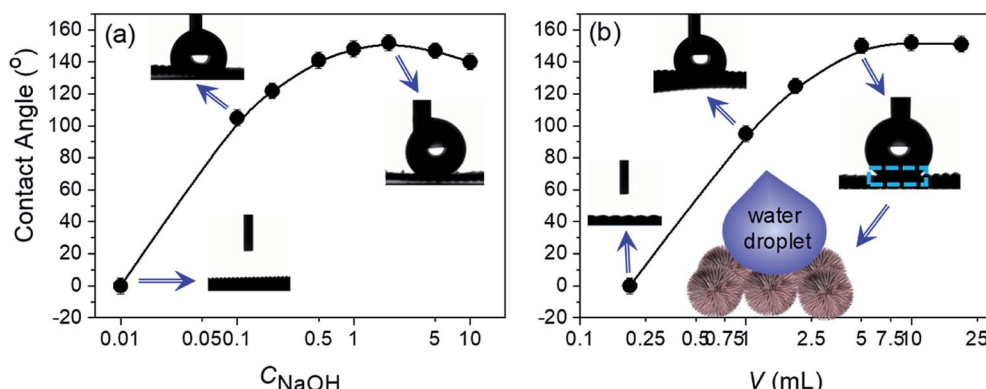
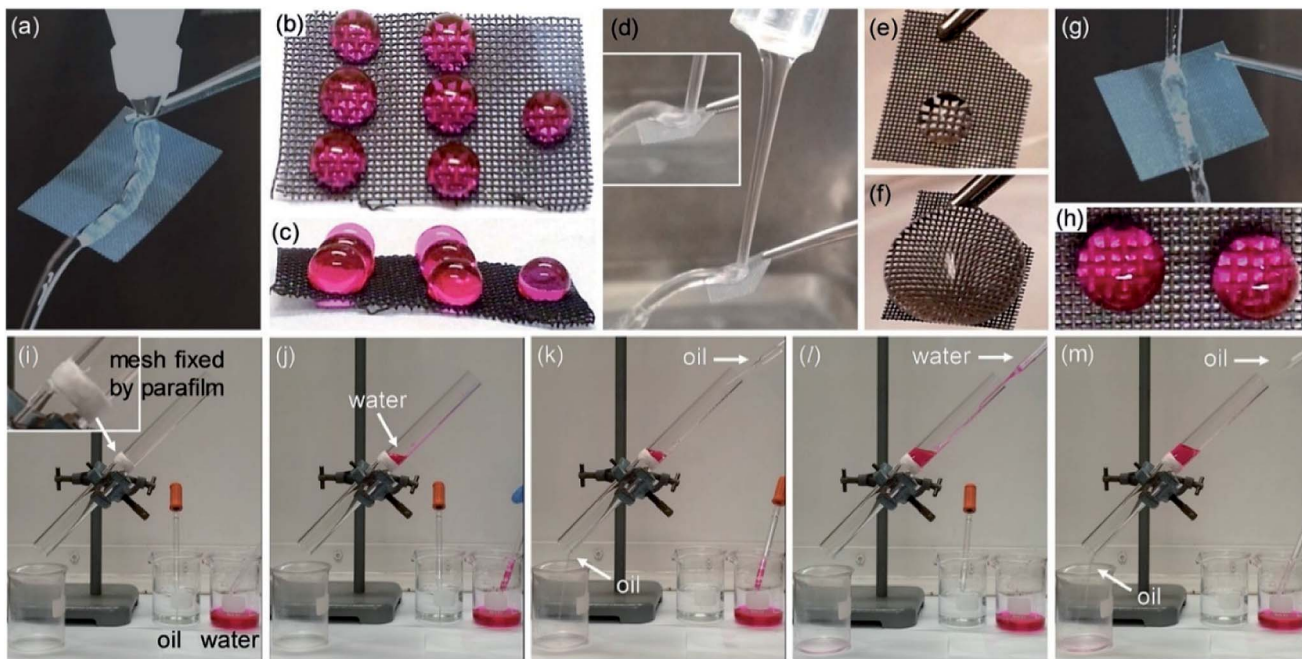


Fig. 3 Demonstration of the wettability properties for the OFP-modified titanate nanostructures on Ti mesh as a function of the NaOH concentration ( $C_{\text{NaOH}}$ ) and modifier concentration ( $C_{\text{OFP}}$ ). (a) Titanate nanostructures synthesized at different  $C_{\text{NaOH}}$  and modified with  $C_{\text{OFP}}$  of 5 mL. (b) Optimal titanate microspheres modified with different  $C_{\text{OFP}}$ . Photographs of water droplets on the titanate-Ti mesh are shown at selected  $C_{\text{NaOH}}$  and  $C_{\text{OFP}}$ . A scheme (inset b) is also proposed to demonstrate the possible surface Cassie state with water-OFP-titanate interfaces.





**Fig. 4** Photograph demonstrations on the superhydrophobic and oil–water separation performances for the OFP-modified titanate microspheres on Ti mesh. (a–c) Wettability of tap–water flow and droplets. (d–f) Wettability of NaCl/KCl solution flow and droplets. (g and h) Wettability of tap–water flow and droplets after oil–water separation. (i–m) Oil–water separation process. Note that the oil used in experiments is dichloromethane ( $\text{CH}_2\text{Cl}_2$ ) and the water showing reddish colour is with Rhodamine B dissolved for clear indicator.

the oil–water separation performance when considering a big difference in surface tension between water ( $72.8 \text{ mN m}^{-1}$ ) and oil ( $<30 \text{ mN m}^{-1}$ ). The superhydrophobic mesh was fixed in between two glass tubes by a parafilm (Fig. 4i). It is noted that the oil used in experiments is dichloromethane ( $\text{CH}_2\text{Cl}_2$ ) and to vividly observe the separation result, Rhodamine B was dissolved into water with showing reddish colour as the indicator (Fig. 4i). Fig. 4j–m show the oil–water separation process. Because of the superhydrophobicity, the water cannot penetrate the Ti mesh but staying on the mesh (Fig. 4j). When further adding the oil ( $\text{CH}_2\text{Cl}_2$ ), it was found that the oil would separately penetrate the mesh but does not affect the water state which still stayed on the mesh. Similar effects were observed when continuing adding water and/or oil into the glass tube. As a result, the oil–water separation performance was steadily achieved as the dynamic process can be seen in video in ESI V3.† After oil–water separation, the OFP-modified titanate microspheres on Ti mesh still exhibit similarly superhydrophobic property (Fig. 4g and h). This suggests that the microstructures and surface Cassie state have not been destroyed, indicating the robust and stable superhydrophobic feature.

As is well known, the surface chemical composition determines the hydrophobic or hydrophilic feature, while the surface morphology and structures further govern the possible superhydrophobicity or superhydrophilicity.<sup>18,19,28–30</sup> The unmodified titanium-based oxide like the present titanate nanostructures, due to their surfaces always terminated by one or more layers of hydroxyl groups, are hydrophilic. It is therefore quite clear that both the chemical modifications and microsphere hierarchical

structures play an important role in superhydrophobicity but the decisive role in hydrophobicity originates from the latter. This is evidenced from Fig. 3 where only the well-defined titanate hierarchical microspheres with appropriate modification could give rise to the superhydrophobicity with high contact angle (CA).

## 4. Conclusion

In summary, an *in situ* “nucleation-cum-growth” solution chemistry route was proposed to synthesize titanate nanowire-assembled hierarchical microspheres on titanium (Ti) mesh *via* a hydrothermal process by controlling surface acidification and subsequently tuning the NaOH concentrations. These directly grown microspheres crystallized in sodium titanate  $[\text{Na}_{1.8}\text{Ti}_{1.95}\square_{0.05}\text{O}_{4.8}]$  ( $\square$  ~ vacancy) with an orthorhombic lepidocrocite layered structure. An individual microsphere has the uniform size of around 10 microns while the constituent nanowires have a diameter of 100 nm growing along [110] orientation. These titanate nanowire-assembled microspheres, due to the specially hierarchical structures on Ti mesh, could achieve the superhydrophobicity through 2,2,3,3,4,4,5,5-octafluoro-1-pentanol (OFP) surface modification. Such robust hierarchical structures were further applied to demonstrate the stable and effective oil–water separation performances. This work presents an integrated strategy of *in situ* “nucleation-cum-growth” synthesis and facile functionalization towards superhydrophobicity for oil–water separation, which might extend to a broad variety of oxide nanowire systems to fabricate



superstructures for wettability tailoring and multi-functional applications.

## Conflicts of interest

There are no conflicts to declare.

## Acknowledgements

This work was supported by the National Key R&D Program of China (Grant No. 2017YFB0406300), Natural Science Foundations of China (Grant No. 51702281, 21773205), Key R&D program of Yunnan Province (Grant No. 2018BA068). W. H. thanks the “One Thousand Youth Talents” Program of China.

## Notes and references

- 1 B. Bolvardi, J. Seyfi, I. Hejazi, M. Otadi, H. A. Khonakdar and S. M. Davachi, *Appl. Surf. Sci.*, 2019, **492**, 862–870.
- 2 X. Xu, F. Dong, X. Yang, H. Liu, L. Guo, Y. Qian, A. Wang, S. Wang and J. Luo, *J. Agric. Food Chem.*, 2019, **67**, 637–643.
- 3 J. Cui, Z. Zhou, A. Xie, Q. Wang, S. Liu, J. Lang, C. Li, Y. Yan and J. Dai, *J. Membr. Sci.*, 2019, **573**, 226–233.
- 4 J. Jiang, Q. Zhang, X. Zhan and F. Chen, *Chem. Eng. J.*, 2019, **358**, 1539–1551.
- 5 F. Li, Z. Wang, S. Huang, Y. Pan and X. Zhao, *Adv. Funct. Mater.*, 2018, **28**, 1–7.
- 6 H. X. Chen, H. M. Tang, M. Duan, Y. G. Liu, M. Liu and F. Zhao, *Environ. Technol.*, 2015, **36**, 1373–1380.
- 7 W. Bigui, Y. Cheng, L. Jianlin, W. Gang, D. Liang, S. Xiaosan, W. Fuping, L. Hua and C. Qing, *Sep. Purif. Technol.*, 2019, **229**, 115808.
- 8 M. J. Nine, S. Kabiri, A. K. Sumona, T. T. Tung, M. M. Moussa and D. Losic, *Sep. Purif. Technol.*, 2020, **233**, 116062.
- 9 N. Li, Q. Yue, B. Gao, X. Xu, R. Su and B. Yu, *J. Cleaner Prod.*, 2019, **207**, 764–771.
- 10 Z. Xue, S. Wang, L. Lin, L. Chen, M. Liu, L. Feng and L. Jiang, *Adv. Mater.*, 2011, **23**, 4270–4273.
- 11 W. Hu, Y. Yu, H. Chen, K. Lau, V. Craig, F. Brink, R. L. Withers and Y. Liu, *Appl. Surf. Sci.*, 2015, **357**, 2022–2027.
- 12 Y. Yu, H. Chen, Y. Liu, V. Craig, L. H. Li and Y. Chen, *Adv. Mater. Interfaces*, 2014, **1**, 1–5.
- 13 H. Shi, Y. He, Y. Pan, H. Di, G. Zeng, L. Zhang and C. Zhang, *J. Membr. Sci.*, 2016, **506**, 60–70.
- 14 M. Tao, L. Xue, F. Liu and L. Jiang, *Adv. Mater.*, 2014, **26**, 2943–2948.
- 15 G. J. Dunderdale, M. W. England, T. Sato, C. Urata and A. Hozumi, *Macromol. Mater. Eng.*, 2016, **301**, 1032–1036.
- 16 R. Ou, J. Wei, L. Jiang, G. P. Simon and H. Wang, *Environ. Sci. Technol.*, 2016, **50**, 906–914.
- 17 Y. Liu, S. Tas, K. Zhang, W. M. De Vos, J. Ma and G. J. Vancso, *Macromolecules*, 2018, **51**, 8435–8442.
- 18 K. Yin, D. Chu, X. Dong, C. Wang, J. A. Duan and J. He, *Nanoscale*, 2017, **9**, 14229–14235.
- 19 D. Qian, D. Chen, N. Li, Q. Xu, H. Li, J. He and J. Lu, *J. Membr. Sci.*, 2018, **554**, 16–25.
- 20 N. T. K. Thanh, N. Maclean and S. Mahiddine, *Chem. Rev.*, 2014, **114**, 7610–7630.
- 21 A. Lafuma and D. Quéré, *Nat. Mater.*, 2003, **2**, 457–460.
- 22 H. Miao, X. Hu, Y. Shang, D. Zhang, R. Ji, E. Liu, Q. Zhang, Y. Wang and J. Fan, *J. Nanosci. Nanotechnol.*, 2012, **12**, 7927–7931.
- 23 T. Kasuga, *Thin Solid Films*, 2006, **496**, 141–145.
- 24 Q. Xue, W. Liu and Z. Zhang, *Wear*, 1997, **213**, 29–32.
- 25 T. Sasaki, M. Watanabe, Y. Michiue, Y. Komatsu, F. Izumi and S. Takenouchi, *Chem. Mater.*, 1995, **7**, 1001–1007.
- 26 Y. B. Mao and S. S. Wong, *J. Am. Chem. Soc.*, 2006, **128**, 8217–8226.
- 27 J. Wang, G. Mao, C. K. Ober and E. J. Kramer, *Macromolecules*, 1997, **30**, 1906–1914.
- 28 N. Selvakumar, H. C. Barshilia and K. S. Rajam, *J. Appl. Phys.*, 2010, **108**, 013505.
- 29 L. Feng, Y. Zhang, J. Xi, Y. Zhu, N. Wang, F. Xia and L. Jiang, *Langmuir*, 2008, **24**, 4114–4119.
- 30 B. Wang, W. Liang, Z. Guo and W. Liu, *Chem. Soc. Rev.*, 2015, **44**, 336–361.

